Charge exchange in 3–30 keV H^+ scattering off clean and AlF_3-covered Al(111) surfaces I. Experimental study

J. O. Lugo,* E. C. Goldberg,[2] E. A. Sánchez,[1] and O. Grizzi[1]
[1]*Céntro Atómico Bariloche, CNEA, CONICET, Instituto Balseiro, UNC, 8400 S. C. de Bariloche, Río Negro, Argentina*
[2]*Instituto de Desarrollo Tecnológico para la Industria Química (CONICET-UNL), and Facultad de Ingeniería Química, UNL, cc91, 3000 Santa Fe, Argentina*

(Received 14 December 2004; revised manuscript received 14 April 2005; published 11 July 2005)

Ion scattering spectroscopy with time-of-flight analysis has been used to study the deposition of a thin AlF_3 insulating film on an Al(111) sample, and to measure the ion fractions for 3–30 keV H^+ projectiles scattered off both the metallic and the insulating surface. The total ion fraction measured for the clean surface at a scattering angle of 108° is $\Gamma \sim 12\%$, composed mainly of negative ions. For AlF_3 film thickness greater than 2 ML, the ion fraction increases, being in this case mainly composed of positive ions ($\Gamma^+ = 35\%$, $\Gamma^- = 3\%$). These changes are interpreted in terms of a competition of resonant electron capture and loss processes between surface and hydrogen electron states.

DOI: 10.1103/PhysRevB.72.035432 PACS number(s): 79.20.Rf, 34.70.+e

I. INTRODUCTION

Collisions of fast atoms and ions with insulator surfaces have received increasing attention in the last years. In particular, studies of photon[1,2] and electron[3–7] emission, sputtering[8] and charge transfer[9–11] have been performed on ionic crystals, such as oxides[12,13] and fluoride compounds.[14,15] In the case of AlF_3, the film growth and its response to ion and electron bombardment are of interest because of the possible applications as resist mask in lithography,[16] the manufacture of metal pads and wires in three dimensions,[17] and high temperature metallic Coulomb blockade devices.[18,19] In addition, from the chemical point of view, AlF_3 plays an important role in many areas of human activity,[20] such as a matrix for trapping and long term storage of hydrogen radicals at ambient temperature.[21]

The specific case of charge exchange processes taking place during the interaction of 0.5–25 keV proton scattering off MgO and LiF surfaces under grazing incidence and observation angles (scattering angles lower than 7°) have been studied by several groups.[6,13,22] These works show that the formation of negative ions (H^-) is strongly increased for insulator surfaces as compared with metallic surfaces like Mg and Al. At very low proton energies (10 eV to 1 keV) and large scattering angles (160°), the charge fraction measured on different ionic compounds like LiCl and $SrTiO_3(001)$ shows an increase of the positive ion fraction when compared with the metallic Pt(111) surface.[11,23] At higher proton energies (50–340 keV) and scattering angles of about 45°, the charge fraction measured for protons scattered off plastic samples such as polystyrene, polycarbonate, etc. is also dominated by positive ions.[24]

On metal surfaces, different mechanisms such as resonant electron transfer (neutralization and ionization)[25–27] and Auger processes[28,29] have been invoked to interpret the final charge states observed in measurements.[15] Resonant processes are possible because the proton ionisation and affinity levels are shifted by the image charge and can be resonant with the empty and occupied levels of the wide solid valence band even at relatively large proton-to-surface distances. The competition of these processes will depend on the scattering conditions and proton incoming and outgoing energies. In the case of insulator surfaces, the contribution of each exchange process to the final charge state is expected to be strongly modified by the characteristics of the insulator electronic states, i.e., large band gaps and narrow valence bands.

In this work we first present results on the characterisation of AlF_3 thin film growth on clean Al(111) using direct recoil spectroscopy with time of flight analysis (TOF-DRS) and Auger electron spectroscopy (AES). For these films we then report measurements of the ion fractions in collisions of 3–30 keV H^+ ions scattered at large scattering angles (108°) and compare them with those for the clean Al substrate. For the Al case, the total ion fraction is composed mainly of negative ions, while for the AlF_3 thin film the total ion fraction strongly increases, being in this case mainly composed of positive ions. These trends can be reproduced by a calculation of resonant electron transfer mechanisms involving the surface band states and the hydrogen levels, as it is presented in the paper following this one.[30]

II. EXPERIMENTAL DETAILS

The experiments were conducted in an ultrahigh-vacuum chamber connected to an ion accelerator working from 1 to 100 keV.[31–33] The ion beams were produced in a radio-frequency source, mass-analysed by a magnet, and finally collimated with several movable slits to spots selected in the range from 0.5 to 4 mm, with a typical angular divergence of 0.1°. For time-of-flight (TOF) measurements the ion beam was pulsed with pairs of parallel plates at frequencies in the range of 10–50 kHz, resulting in resolution times of ~100 to 500 ns for proton energies from 3 to 30 keV, respectively.

The main chamber, which will be described in detail elsewhere, has two TOF spectrometers that allow discrimination of neutral, negative and positive particles (Fig. 1). One of these spectrometers can be rotated inside the UHV chamber in order to select the scattering angle θ in the range from 0 to

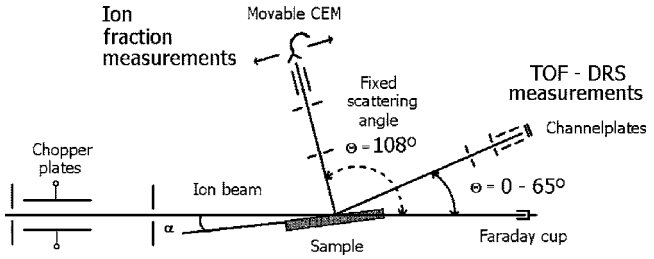

FIG. 1. Schematic of the ion scattering geometry. See text for details.

65° with an angular acceptance of $\Delta\theta = \pm 1°$, defined by two rectangular slits (2×10 mm). The particles passing through these slits are deflected according to their charge state by two pairs of parallel plates, and are then detected by three electrodes placed behind two channelplates in a chevron configuration. The sample to channelplate flight path is 0.75 m.

The other TOF spectrometer consist of a channeltron electron multiplier (CEM) located at the end of a 1.02 m length drift tube fixed at a scattering angle of 108°. In front of the CEM there is a pair of parallel plates that allows deviation of charged particles by applying a voltage between them. The charge fraction of the scattered particles can be measured by scanning the CEM in front of the deflecting plates.

The electron energy distributions for AES were measured with a custom-made cylindrical mirror spectrometer placed in other UHV system[33] working at 1% energy resolution and ±2° angular resolution. The inner cylinder of the spectrometer has a small exit hole (instead of using the full symmetry of the analyzer) and rotates around its main axis allowing measurements in a wide range of observation angles. For the present measurements the observation angles were fixed at 49.3° of elevation angle with respect to the surface and 36.2° with respect to the scattering plane.[34] The electron beam incidence angle was 34° with respect to the surface plane.

The sample is mounted on manipulators allowing independent and continuous variation of the ion incident direction with respect to the surface plane (α) and to a main crystallographic surface axis (ϕ).

The substrate was prepared by cycles of 20 keV grazing Ar^+ bombardment ($\sim 2°$) and annealing at 450 °C. This method produces very flat surfaces as has been shown in previous works.[10,35,36]

Fluoride depositions were performed in situ from a Knudsen cell charged with anhydrous AlF_3.[37] The cell was carefully degassed and shuttered to avoid sample contamination. UHV conditions (10^{-10} Torr range) were kept throughout the evaporation. The same Knudsen cell was used in both UHV systems keeping similar conditions for the evaporation [the same Al(111) sample, and the same sample-to-evaporator distance and temperature]. The base pressures in the collision chambers were about 2 to 5×10^{-10} Torr and remained in the 10^{-10} Torr range when the ion beam line was open. The surface cleanliness was verified by TOF-DRS and AES before and after deposition.

The characterization of the AlF_3 deposition with TOF-DRS was performed by measuring the direct recoiled particles detected by the rotatable TOF spectrometer at a fixed scattering angle of 30°. The bombardment was performed by 4.2 keV Ar^+ ions impinging at an incident angle α (with respect to the surface) of 15°. The charge fraction for H^+ projectiles scattered at 108° was measured with the fixed TOF spectrometer at $\alpha = 15°$, with primary energies between 3 to 30 keV.

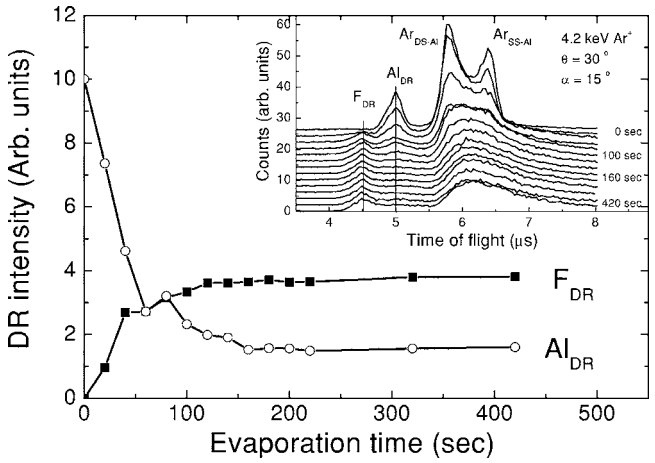

FIG. 2. Al and F DR intensities measured as a function of the AlF_3 evaporation time. Inset: the corresponding TOF-DRS spectra measured during the deposition of AlF_3 on Al(111).

III. RESULTS

A. Study of AlF_3 film growth by TOF-DRS

In the inset of Fig. 2 we show the TOF-DRS spectra measured after deposition of AlF_3 on clean Al(111) at room temperature. We observe that after evaporation, the Al direct recoil (DR) peak intensity decreases while the F DR peak intensity increases reaching a steady value. In Fig. 2 we show the corresponding intensities obtained from integration of the peaks shown in the inset of Fig. 2, after correction with the scattering cross sections from Robinson tables.[38] The intensities are normalized by setting a value of 10 for the clean Al DR signal. The F (Al) DR signal increases (decreases) and reaches a plateau for deposition times of about 120–160 s. At the end of the evaporation, the ratio (F/Al) of these peak intensities is about 2.4. Other measurements performed at larger scattering angles suggest a ratio value of 3. The TOF spectra were also measured as a function of the sample azimuthal orientation, keeping the incidence angle fixed. Figure 3 shows these results for clean Al(111) and after deposition of ~ 3 ML of AlF_3. Note that while the Al DR intensity for clean Al(111) shows strong variations produced by focusing and shadowing effects on the scattering of the Ar ions off the well-ordered Al single crystal, the F and Al DR intensities measured on the AlF_3 covered surface present almost no variation, indicating that there is no long-range order in the film. Assuming that there is no preferential focusing in the noncrystalline film, the ratio of the intensities suggests that there are about 2–3 F atoms on the surface per each Al atom. In a previous characterization performed for the growth of AlF_3 on GaAs(110) using Kr ions at larger scattering angles[37] we found that this ratio was closer to 3,

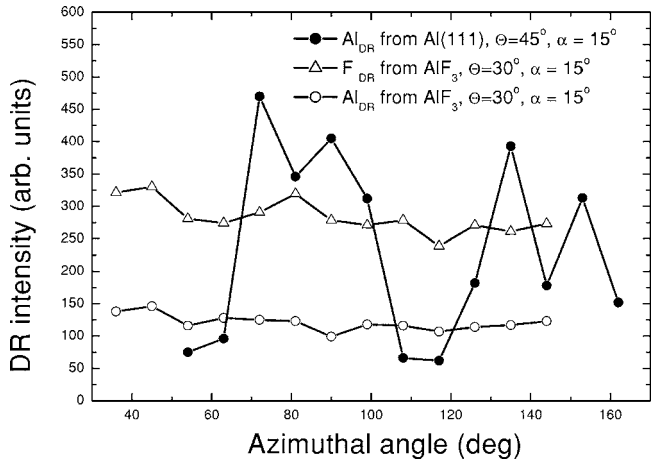

FIG. 3. Intensity of Al and F DR peaks measured with 5 keV Ar^+ scattered on AlF_3 and on Al(111) samples.

i.e., the expected value for the stoichiometric case. This ratio is difficult to obtain with TOF-DRS mainly due to the uncertainties in the subtraction of the multiple scattering background present below the DR peaks. To our knowledge, the composition and crystallography of thin AlF_3 films is not known. The model used to describe the surface in the calculation of paper II assumes neutrality of the surface of the ionic crystal, and has a ratio of F to Al atoms equal to 2 (paper following this one[30]).

In Fig. 4, the peak-to-peak Auger intensities for F (647 eV) and for the metallic Al° (68 eV) are shown as a function of the AlF_3 evaporation time.[3] The F Auger intensity increases, while the metallic Al° intensity, that comes from the Al(111) substrate, decreases and disappears for evaporation times greater than 400 s. At this coverage, the only Al signal observed in the Auger spectrum is located around 48 eV, corresponding to the Al^{+3} Auger signal coming from completely oxidized Al atoms (see inset of Fig. 4). The disappearance of the substrate signal for evaporation times higher than 400 s indicates that the film completely covers the substrate. In this condition, the substrate Auger electrons should

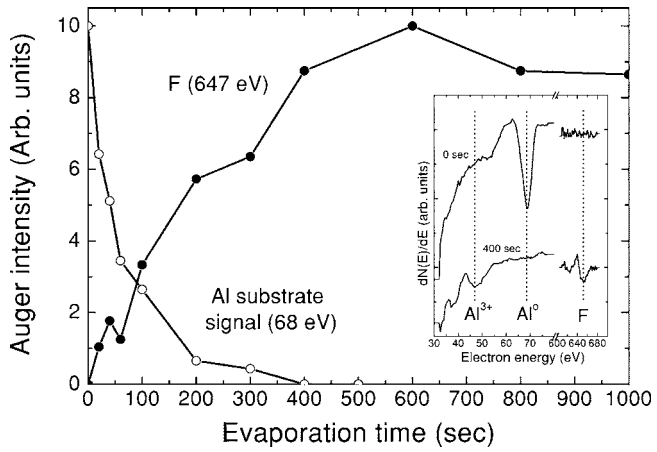

FIG. 4. Peak-to-peak Auger intensities measured as a function of the AlF_3 evaporation time. Inset: Auger electron spectra for the clean Al surface and the AlF_3 covered surface.

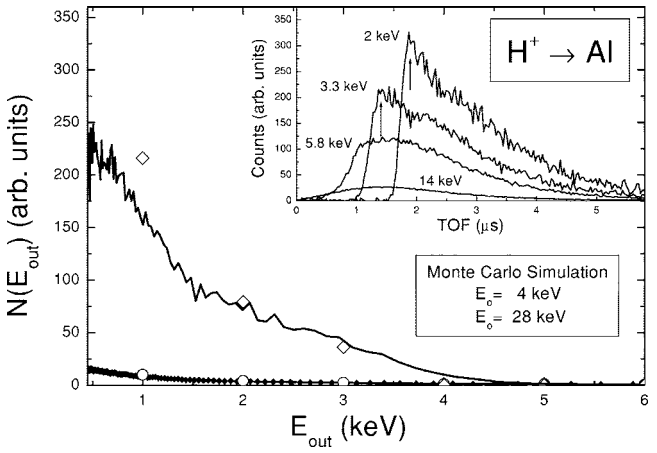

FIG. 5. Comparison of the energy distributions obtained from TOF spectra with Monte Carlo simulations for 4 (open diamond) and 28 keV H^+ (open circle). Inset: Total (N+I) TOF spectra of H scattered off a clean Al(111) surface.

traverse a length through the film of about 4 times its mean free path. The mean free path estimated from Ref. 38 for 68 eV electrons moving in an homogeneous AlF_3 sample is about 6 Å.[39] Since, on average, the electrons traverse the film at an angle of 35.2° with respect to the surface plane, the thickness of the film in the direction perpendicular to sample should be about 13.4 Å. In the AlF_3 single crystal the Al-Al separation is 3.5 Å.[40] So, the thickness of the AlF_3 film, for an evaporation time of 400 s, should correspond to about 3–4 monolayer (ML). This estimation, and the saturation of the F and Al DR intensities for evaporation times of about 120–160 s, suggests the formation of 1 ML of AlF_3 for evaporation times of the order of 100–150 s (along the work we used 120 s as equivalent to 1 ML). The saturation of the F DR intensity at smaller coverages than those observed for the F peak-to-peak Auger signal reflects the higher sensitivity to the topmost layer of TOF-DRS over AES.

Previous measurements by electron energy loss spectroscopy (EELS) for AlF_3 on Al(111) showed[3] that the dielectric response of very thin films (~3 ML) is similar to the calculated one for bulk AlF_3. The results presented here, together with those presented previously,[3,41] indicate that the film grown at room temperature covers completely the substrate, presenting no long-range crystallographic order, and electronic properties similar to those of bulk AlF_3 materials. A topographic characterization performed on about 50 ML AlF_3 film with an atomic force microscope shows that the roughness in 1×1 μm areas is lower than 18 Å. This indicates that, even for relatively thick films, the surface topography is rather flat.

B. Backscattering of H^+ projectiles

As it was mentioned in Sec. II, the scattering of hydrogen atoms off clean and AlF_3 covered Al(111) surfaces was studied for a fixed backscattering condition ($\Theta=108°$, $\alpha=15°$). In the inset of Fig. 5 we present the total (ion+neutral) TOF spectra measured for H^+ projectiles on a clean Al sample with energies Eo in the range from 2 to 14 keV. The TOF

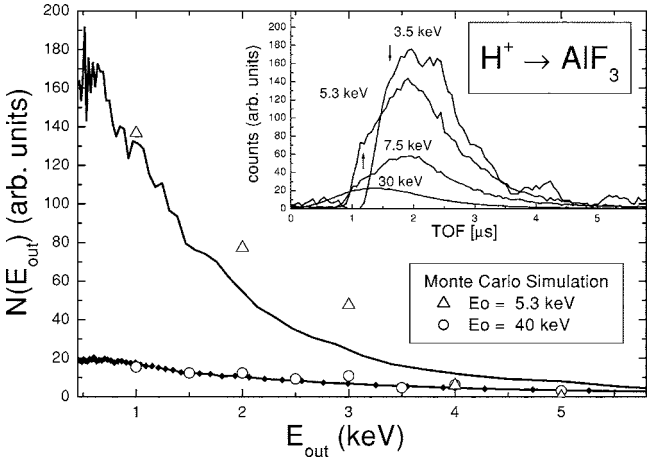

FIG. 6. Comparison of the energy distributions obtained from TOF spectra with Monte Carlo simulations for 5.3 (open diamond) and 40 keV H^+ (open circle). Inset: Total (N+I) TOF spectra of H scattered off AlF_3 deposited on Al(111).

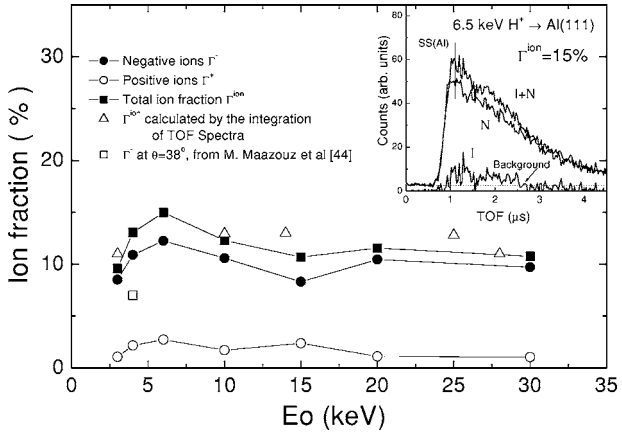

FIG. 7. Negative and positive ion fractions as a function of the incoming projectile energy. Inset: Total ($N+I$), neutral (N) and ion (I) TOF spectra measured for 6.5 keV H^+ scattered off an Al(111) surface.

spectra are smooth distributions, where single scattering peaks can only be distinguished for the lowest incoming energies (see arrows). The spectra corresponding to Eo equal to 4 and 28 keV converted to energy distributions (under the assumption that all the outgoing particles are H atoms) are shown in Fig. 5. The general trends of the energy distributions for different projectile energies are reproduced by a Monte Carlo simulation performed with the SRIM2003 code.[42] This calculation indicates that the particles leaving the surface are mainly H atoms that have had multiple collisions in their incoming and outgoing trajectories inside the solid. These energies distributions are due to elastic and inelastic energy losses suffered by the projectile that have been reflected from about 200 and 500 Å inside the solid, for projectiles energies of 5 and 30 keV, respectively. Similar results were obtained by Agamy *et al.*[43] for the scattered TOF spectra and energy distributions produced by 5 to 15 keV H ions scattered off a Si sample at $\Theta=135°$. The little variation of the energy distribution with the projectile energy is expected because of the large penetration of the projectile inside the solid. In Fig. 6 we show the TOF spectra (inset) and the corresponding energy distributions measured at $\Theta=108°$ for 3.5 to 30 keV H^+ ions incoming at $\alpha=15°$ onto ~3 ML AlF_3 deposited on Al(111). In this case, the single scattering features from Al atoms are less evident. The Monte Carlo simulations performed for the thin insulating film deposited on Al also reproduces the general trends of the energy distributions (Fig. 6).

Although the TOF spectra and the energy distributions measured for Al and AlF_3 surfaces look quite similar, the measured charge states of the scattered H atoms differ strongly as it is shown in the next section.

C. Charge fractions in backscattered H^+ projectiles

In the inset of Fig. 7 the total ($I+N$), neutral (N) and ion (I) TOF spectra measured for 6.5 keV H^+ bombardment of a clean Al(111) surface are shown. The $N(I+N)$ spectrum was measured by polarizing (grounding) the deflecting plates placed in front of the CEM detector (located at the aligned position). The ion spectrum can be obtained by subtracting those spectra $((N+I)-(N))$. The total ion fraction (positive plus negative) is given by the ratio $\Gamma^{ion}=(\text{area}(N+I)-\text{area}(N))/\text{area}(N+I)$, obtained from the integration of the total area of each spectrum (after removing a linear background). For 6.5 keV H^+ on Al(111) the ion fraction results $\Gamma^{ion}=15\%$. Since the background contribution is small, and mainly coming from survival neutrals in the beam line, the ion fractions can be measured with a *continuous* beam, i.e., as the total amount of particles that hit the CEM, with and without polarisation of the deflecting plates. This method gives the total ion fractions very rapidly, and with better statistic. The values obtained in this way were similar to those obtained from the measurement of the TOF spectra.

In order to get information about the production of negative and positive charge fractions, the CEM was scanned in front of the polarized deflecting plates, from one side to the other side of the aligned position, under continuous ion bombardment. In Fig. 7 we show the positive (Γ^+), the negative (Γ^-) and the total (Γ^{ion}) ion fraction as a function of the incoming projectile energy (from 3 to 30 keV). The analysis of the outgoing charge states shows that the main contribution to the total ion fraction for the clean Al surface comes from negative ions, with $\Gamma^-\sim 10\%$, whereas the positive ion fraction Γ^+ is about 2%. We have also included in Fig. 7 the total ion fraction calculated from some TOF spectra. No remarkable variations have been observed above 7 keV, at lower energies there is an increase of the ion fraction for proton energies from 3 to 6 keV. A similar behavior has been observed by Bhattacharya *et al.*[44] for the backscattering ($\Theta=135°$) of H^+ and D^+ atoms from several polycrystalline substrates. The formation of H^- in Al was studied previously by Maazouz *et al.*[45] at energies from 1 to 4 keV, and at different projectile incidence ($3°<\alpha<33°$) and scattering ($\Theta=7°$ and $\Theta=38°$) angles. They showed that the negative ion fraction increased when the exit angle($\varphi=\Theta-\alpha$) increased, reaching a value of ~6% for $\varphi=33°$, being at this

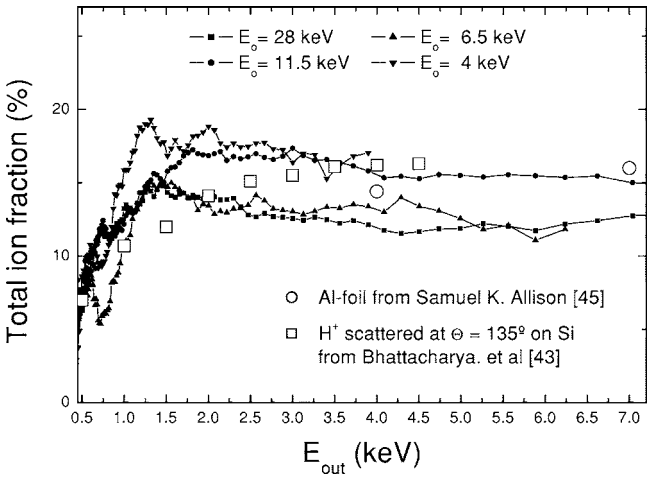

FIG. 8. Point-by-point total (positive and negative) ion fractions calculated from TOF spectra for H ions scattered off an Al(111) surface.

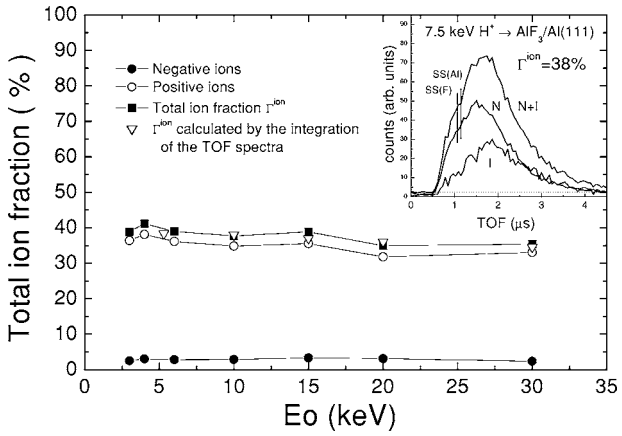

FIG. 9. Negative (solid circle), positive (open circle), and total (solid square) ion fractions obtained in the continuous beam mode as a function of the incoming projectile energy, (solid down triangle) total ion fraction obtained from integration of TOF spectra. Inset: Total ($N+I$), neutral (N) and ion (I) TOF spectra measured for 7.5 keV H^+ scattered off an AlF_3 surface.

condition barely dependent on the incident energy. Our present results agree with this general behavior, at larger observation angles (in our conditions, $\varphi=93°$) the negative ion fraction increases up to 10% and becomes essentially independent of the incoming energy above 10 keV.

To obtain information about the dependence of the total ion fraction with the outgoing projectile energy (E_{out}) we have converted the TOF spectra to energy distributions, and have calculated the ion fraction point-by-point from these distributions as it is shown in Fig. 8. The total ion fraction increases from ~5% for 0.5 keV, and reaches a constant value of 14–18% for E_{out} greater than 1.5 keV. This behavior is similar to that reported by Bhattacharya *et al.*[44] for backscattering of H^+ ions on Si polycrystalline samples, and to that measured by S. K. Allison[46] for transmission of H ions through thin self-supported Al foils (Fig. 8).

As it was mentioned previously, different mechanism such as resonant electron transfer and Auger processes have been invoked to explain the experimental results in previous measurements.[10,13,25–29] In the present case of large scattering angle, we describe the experimental results in terms of a calculation using a time-dependent formalism that accounts for the resonant charge exchange between the projectile and the surface occurring during the outgoing trajectory of the emitted particle. Details of the calculation are reported in the paper following this one.[30] Briefly, an Anderson-type Hamiltonian within a spinless approach was used, the atom-surface interaction was calculated by using a Hartree-Fock approximation, and the extended features of the surface were accounted by an appropriate description of the local density of states. The calculation was performed by assuming initially either neutral or negative charge states for H at a position near the surface, from where the dynamical evolution was followed through a time-dependent Green's function formalism.[47] The H^- formation from H^0 and the H^- survival ($P^-_{(-)}$) of an initially negative charged hydrogen by a resonant exchange process, were calculated by considering the affinity level as the only one H active level. The H^+ formation from H^0 was also calculated by assuming in this case that the active level in the charge transfer process is the H ionization level. The calculation shows that both initial charge state configurations lead to the same final ion fractions; $\Gamma^+\sim 3\%$ and $\Gamma^-\sim 9\%$, values that are close to the experimental ones.[30]

In the inset of Fig. 9 the total ($I+N$), neutral (N) and ion (I) TOF spectra measured for 7.5 keV H^+ bombardment of a clean Al(111) surface covered by about 3 ML AlF_3 are shown. Similar spectra are observed for coverages larger than 10 ML. The total ion fraction obtained from the integration of the TOF spectra is about 38%, i.e., it has increased by more than twice with respect to the clean Al surface.

In order to get information about the main charge state of the H atoms receding off AlF_3 we measured the negative and positive charge fractions (from 3 to 30 keV) by scanning the CEM in front of the deflecting plates. These results are shown in Fig. 9 together with the total ion fraction calculated from the TOF spectra. In the present case, the increase of the total ion fraction from about 12 to 38% when the surface goes from metallic Al to oxidized Al, corresponds to a decrease of the negative ion fraction from 10 to 3% (on the average), and an increase of the positive ion fraction from 2 to 35%, respectively. On the other hand, like in the case of Al surfaces, no remarkable variations have been observed for different incoming energies, just a small decrease from 40 to 35% for proton energies from 3 to 30 keV.

Increases of the negative charge fraction for different ionic surfaces have been reported for hydrogen energies lower than 6 keV and grazing incidence and observation geometry.[13,15,48] For the case of large scattering angles ($\Theta=38°$), Ustaze *et al.*[13] reported that Γ^- is about 9% for either MgO or Mg. In the case of Al oxidation the negative ion fraction for 4 keV H projectiles scattered at $\Theta=38°$ increases from 3 to 4.5%.[48] On the other hand, increases of the positive ion fractions when compared with the metallic surfaces have been observed at large scattering angles for other ionic compounds[11,23] and plastic surfaces.[24]

In Fig. 10 we show the total ion fraction as a function of the outgoing H energy, obtained point-by-point from the en-

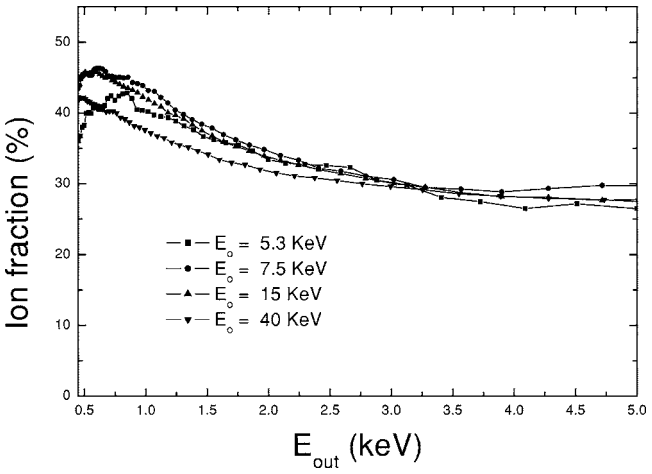

FIG. 10. Point-by-point total ion fraction calculated from TOF spectra for H ions scattered off ~3 ML AlF_3 deposited on Al(111).

ergy distributions derived from the TOF spectra. Note that the energy dependence is different when compared with the clean Al(111) case. The total ion fraction decreases from ~40% for 0.5 keV to 30% for E_{out} greater than 3 keV. Measurements performed for grazing scattering of H^+ ions on LiF(100) surfaces by Auth *et al.*[15] show a decrease, but with the maximum of the negative ion fraction of ~7% at ~2 keV.

The increase of the negative ion fraction in experiments of grazing scattering of H ions on insulator surfaces was interpreted in terms of a model of local electron capture from negatively charged sites of an ionic crystal where the interplay of capture of localized electrons in binary-type collision events close to the surface, and the subsequent suppression of the electron loss due to the large band gap of the sample, defines the final ion fraction.[13,15,18] In our case, where detection of H atoms is performed at large scattering angles ($\Theta = 108°$), for large incident angles ($\alpha = 15°$), one should take into account the deep penetration of the projectile before leaving the surface. Due to the specific electronic characteristics of the ionic film (low electron mobility, localized electron states, large band gap), the charge state of H atoms that had traversed the last layers of the insulating film is assumed to be positive. Under this assumption the final charge fraction is determined by the electron capture from $2p$ F states (valence band) to the H ionization level during the dynamical evolution of the receding atom. This scenario is supported by the theoretical results presented in the paper following this one[30] that reproduces the general trends of the experimental results shown in the present work.

IV. SUMMARY AND CONCLUSIONS

In this paper we presented an extension of the experimental studies of Ref. 40 for the scattering of H ions off metallic Al(111) clean and covered with an insulator thin film (AlF_3). The direct recoiling signals (Al and F) excited by Ar bombardment, together with AES and EELS measurements, were used to characterize the growth of AlF_3 thin films on Al(111). The ion fractions for 3–30 keV H^+ scattering at 108° off both the clean and AlF_3 covered Al(111) surfaces was measured. The experimental results show a strong increase of the positive ion fraction, from ~2% for clean Al(111), to ~35% for AlF_3; and a decrease of the negative ion fraction, from~10 to ~3%. This dependence is compatible with a resonant charge transfer between the solid and the hydrogen projectile, which has different initial charge states at the moment of leaving the metallic and the ionic surface. A calculation that takes into account the valence band levels and the core levels describes the general trends of the experiment in both surfaces. Details of the model and a discussion of the origin of the contributions to the charge fractions are presented in the paper following this one.[30]

ACKNOWLEDGMENTS

We acknowledge Dr. V. A. Vladimir for his participation in the design of different parts of the experimental setup and for useful discussions regarding the experiment. This work was supported by CAI+D 2000 N0 1-6-76 from Universidad Nacional del Litoral, and PIP 02833/99 from CONICET. We acknowledge partial financial support from the ANPCyT (PICTs 03-03579/06249/6325/14452), CONICET (PIP 0423), and Fundación Antorchas (A-13927-17, 14022/111).

*Fellow of Agencia Nacional de Promoción Científica y Tecnológica ANPCyT.

[1] H. Winter, C. Auth, and T. Hecht, Vacuum **66**, 137 (2002).
[2] T. Hecht and H. Winter, Phys. Lett. A **243**, 306 (1998).
[3] E. A. Sánchez, G. G. Otero, N. Tognalli, O. Grizzi, and V. H. Ponce, Nucl. Instrum. Methods Phys. Res. B **203**, 41 (2003).
[4] M. L. Martiarena and V. H. Ponce, Nucl. Instrum. Methods Phys. Res. B **203**, 62 (2003).
[5] F. Golek, and E. Bauer, Surf. Sci. **369**, 415 (2001).
[6] P. Roncin, J. Villette, J. P. Atanas, and H. Khemliche, Phys. Rev. Lett. **83**, 864 (1999).
[7] P. A. Zeijlmans van Emmichoven, A. Niehaus, P. Stracke, F. Wiegershaus, S. Krischok, V. Kempter, A. Arnau, F. J. García deAbajo, and M. Penalba, Phys. Rev. B **59**, 10950 (1999).
[8] K. Morita and A. Yoshii, Nucl. Instrum. Methods Phys. Res. B **203**, 239 (2003).
[9] A. G. Borisov and V. A. Esaulov, J. Phys.: Condens. Matter **12**, R177 (2000).
[10] H. Winter, Phys. Rep. **367**, 387 (2002).
[11] R. Souda, K. Yamamoto, W. Hayami, B. Tilley, T. Aizawa, and Y. Ishizawa, Surf. Sci. **324**, L349 (2001).
[12] R. Souda, K. Yamamoto, W. Hayami, T. Aizawa, and Y. Ishizawa, Phys. Rev. B **50**, 4733 (1994).
[13] S. Ustaze, R. Verucchi, S. Lacombe, L. Guillemot, and V. A.

Esaulov, Phys. Rev. Lett. **79**, 3526 (1997).
[14] C. Auth, A. G. Borisov, and H. Winter, Phys. Rev. Lett. **75**, 2292 (1995).
[15] C. Auth, A. Mertens, H. Winter, A. G. Borisov, and V. Sidis, Phys. Rev. A **57**, 351 (1998).
[16] G. S. Chen, C. B. Boothroyd, and C. J. Humphreys, Appl. Phys. Lett. **69**, 170 (1996).
[17] A. Muray, M. Scheinfein, and M. Isaacson, J. Vac. Sci. Technol. B **3**, 367 (1985).
[18] C. Vieu, M. Mejias, F. Carcenac, G. Faini, and H. Launois, Microelectron. Eng. **30**, 403 (1996).
[19] J. Gierak, A. Septier, and C. Vieu, Nucl. Instrum. Methods Phys. Res. A **427**, 91 (1999).
[20] J. Pinkas, and H. W. Roesky, J. Fluorine Chem. **122**, 125 (2003).
[21] G. Scholz, R. Stosser, J. A. Momand, A. Zehl, and J. Klein, Angew. Chem., Int. Ed. **39**, 2516 (2000).
[22] H. Winter, C. Auth, and A. G. Borisov, Nucl. Instrum. Methods Phys. Res. B **115**, 133 (1996).
[23] R. Souda, K. Yamamoto, W. Hayami, T. Aizawa, and Y. Ishizawa, Phys. Rev. B **51**, 4463 (1995).
[24] G. G. Ross and M. Gauthier, Nucl. Instrum. Methods Phys. Res. B **193** , 449 (2002).
[25] R. Brako and D. M. Newns, Rep. Prog. Phys. **52**, 655 (1989).
[26] J. Los and J. J. G. Geerlings, Phys. Rep. **190**, 133 (1990).
[27] J. W. Rabalais, *Low Energy Ion-Surface Interactions* (Wiley, New York, 1994).
[28] H. Winter and A. G. Borisov, Nucl. Instrum. Methods Phys. Res. B **115** , 211 (1996).
[29] R. Zimny, Z. L. Miskovic, N. N. Nedeljkovic, and Lj. D. Nedeljkovic, Surf. Sci. **255**, 135 (1991).
[30] J. O. Lugo, E. C. Goldberg, E. A. Sánchez, and O. Grizzi, Phys. Rev. B **72**, 035433 (2005).
[31] R. G. Pregliasco, J. E. Gayone, E. A. Sanchez, and O. Grizzi, in *Surface Vacuum and Their Applications*, edited by I. Hernández Calderón and P. Somoza, AIP Conf. Proc. No. 378 (AIP, New York, 1994), p. 84.
[32] J. E. Gayone, R. G. Pregliasco, G. R. Gómez, E. A. Sánchez, and O. Grizzi, Phys. Rev. B **56**, 4186 (1997).
[33] L. F. De Ferrariis, F. Tutzauer, E. A. Sánchez, and R. A. Baragiola, Nucl. Instrum. Methods Phys. Res. A **281**, 43 (1989).
[34] G. R. Gómez, E. A. Sánchez, O. Grizzi, M. L. Martiarena, and V. H. Ponce, Nucl. Instrum. Methods Phys. Res. B **122**, 171 (1997).
[35] G. R. Gómez, E. A. Sánchez, and O. Grizzi, Phys. Rev. B **57**, 12573 (1998).
[36] O. Grizzi, E. A. Sánchez, J. E. Gayone L. Guillemot, V. A. Esaulov, and R. A. Baragiola, Surf. Sci. **260**, 71 (2000).
[37] L. I. Vergara, R. A. Vidal, J. Ferrón, E. A. Sánchez, and O. Grizzi, Surf. Sci. **482–485**, 854 (2001).
[38] *Table of Clasical Scattering Integrals*, edited by M. T. Robinson (Oak Ridge National Laboratory, Oak Ridge, TN, 1970), ORNL-4556, UC-34 - Physics.
[39] M. P. Seah and W. A. Dench, Surf. Interface Anal. **1**, 2 (1979).
[40] Ph. Daniel, A. Bulou, M. Rousseau, J. Nouet, J. L. Fourquet, M. Leblanc, and R. Burriel, J. Phys.: Condens. Matter **2**, 5663 (1990).
[41] J. O. Lugo, E. C. Goldberg, E. A. Sánchez, and O. Grizzi, Phys. Status Solidi A **201**, 2356 (2004).
[42] http://www.srim.org/SRIM/SRIM2003.htm.
[43] S. A. Agamy and J. E. Robinson, Surf. Sci. **90**, 648 (1979).
[44] R. S. Bhattacharya, W. Eckstein, and H. Verbeek, Surf. Sci. **93**, 563 (1980).
[45] M. Maazouz, R Baragiola, A. Borisov, V. A. Esaulov, S. Lacombe, J. P. Gauyacq, L. Guillemot, and D. Teillet-Billy, Surf. Sci. **364**, L568 (1996).
[46] S. K. Allison, Rev. Mod. Phys. **30**, 1137 (1958).
[47] M. C. Torralba, P. G. Bolcatto, and E. C. Goldberg, Phys. Rev. B **68**, 075406 (2003).
[48] M. Maazouz, L. Guillemot, S. Lacombe, and V. A. Esaulov, Phys. Rev. Lett. **77**, 4265 (1996).